

## Supplementary Figures

**Supp. Fig. 1. Sequence alignment of the sequence of the conserved N-terminal region of Orai proteins.** Putative CaM binding domain (blue), conserved region (green) and transmembrane region 1 (red).

**Supp. Fig. 2. Localization of Orai3 deletion mutants.** Confocal fluorescence images from a representative cell expressing a) wild-type YFP-Orai3, b) YFP-Orai3  $\Delta N_{1-47}$ , c) YFP-Orai3  $\Delta N_{1-51}$ , d) YFP Orai3  $\Delta N_{1-53}$ , e) YFP-Orai3  $\Delta N_{1-55}$ , f) YFP-Orai3  $\Delta N_{1-57}$ , g) YFP-Orai3  $\Delta N_{1-62}$  and h) YFP-Orai3  $\Delta N$ -term. i) Block diagram comparing plasma membrane intensities of Orai3, Orai3  $\Delta N_{1-47}$  and Orai3  $\Delta N_{1-57}$ .

**Supp. Fig. 3. Inactivation profile, store-operated and 2-APB-mediated currents of Orai3 deletion mutants.** a) d) Store-operated currents of Orai3  $\Delta N_{1-47}$  and  $\Delta N_{1-55}$ . b) e) Corresponding current/voltage relationships to a) d). c) f) Corresponding fast inactivation to a) d). g) h) 2-APB mediated currents of all Orai3 deletion mutants. i) Store-operated activation of Orai3  $\Delta N_{1-60}$  and  $\Delta N_{1-62}$ . j-l) Fast inactivation upon voltage-steps to -90mV for 1600ms.

**Supp. Fig. 4. Comparison of peptide aa 47-65 and peptide aa 52-65 with respect to CaM binding.** The sensor chip was prepared and cleaned as described (Hahn et al., 2007, Chemical Monthly 138, 245–252) and immediately immersed in an ethanolic solution of octadecanethiol (20  $\mu$ M) for 72 h to form a hydrophobic self-assembled monolayer. After rinsing in ethanol and water, the chip was mounted in the BIAcore setup and superfused with PBS. The flow was 20  $\mu$ l/min (except for lipid vesicle injection which was at 4  $\mu$ l/min) and all injection volumes were 100  $\mu$ l. The surface was washed by injection of octylglucoside (40 mM, 100  $\mu$ l), whereupon lipid vesicles (DOPC/biotin-cap-DOPE/PS at a molar ratio of 7/2/1, 1 mg/ml lipid concentration in PBS) were injected at a flow rate of 4  $\mu$ l/min, yielding a phospholipid monolayer with biotin residues on 20% of the lipid head groups (Sagmeister et al., 2009, Biosens. Bioelectron. 24, 2643-2648). Adhering vesicles were removed by injection of 10 mM NaOH. Then the running buffer was changed to Hepes buffer (150 mM NaCl, 5 mM Hepes, pH 7.3). Streptavidin (2  $\mu$ M, in Hepes buffer) was injected in flow cell 2 yielding a dense layer of streptavidin. The free binding sites were blocked with *D*-biotin (200  $\mu$ M in Hepes buffer). After thorough rinsing of the complete microfluidics system to remove free *D*-biotin, streptavidin was applied to flow cell 1, followed by injection biotin-EG<sub>8</sub>-Orai peptide aa 47-65 or aa 52-65 (2  $\mu$ M in Hepes buffer), also in flow cell 1 only. Then the running buffer was changed to Hepes buffer (150 mM NaCl, 5 mM Hepes, pH 7.3) either containing 2 mM EGTA (Ca-free buffer, data not shown) or to 2 mM CaCl<sub>2</sub> (Ca-buffer) and CaM (2  $\mu$ M) was injected in the corresponding buffer also. The resonance angle change is shown in kiloresonance units (1000 RU, equivalent to a 0.1° change in the resonance angle). Rough estimates of the K<sub>D</sub> values for the binding of CaM to the two peptides were calculated with the BIAevaluation software 3.1 (1:1 Langmuir binding). The sensorgrams show CaM binding of CaM to peptide aa 47-65 (flow cell 1, solid black line) and to the corresponding peptide-free control cell (flow cell 2, dotted black line), as well as of CaM binding to peptide aa 52-65 (flow cell 1, solid red line) and to the corresponding peptide-free control cell (flow cell 2, dotted red line). The curves were vertically displaced by small increments to avoid overlap of the data.

**Supp. Fig. 5. Comparison of peptide aa 47-65 and peptide aa 52-65 R52A R53A with respect to CaM binding.** The sensor chip was prepared and cleaned as described (Hahn et al., 2007, Chemical Monthly 138, 245–252) and immediately immersed in an acetonitrile

solution of N-(14-hydroxy-3,6,9,12-tetraoxatetradecyl)-16-sulfanylhexadecanoylamide (16  $\mu$ M, Svedhem et al. 2001, J. Org. Chem. 66, 4494-4503) and N-(23-biotinamido-3,6,9,12,15,18,21-heptaoxatricosanyl)-16-sulfanylhexadecanoylamide (4  $\mu$ M, Pollheimer et al., manuscript in preparation) for 72 h to form a protein-resistant self-assembled monolayer with biotin on 20% of the oligo(ethylene glycol) chains, in close analogy to Jung et al. (1999, Sensors and Actuators B 54, 137-144). After rinsing in acetonitrile, ethanol, and water, the chip was mounted in the BIAcore setup and superfused with Hepes buffer (150 mM NaCl, 5 mM Hepes, pH 7.3). The selective functionalization of the control cell (flow cell 2) with biotin-blocked streptavidin and of the measuring cell (flow cell 1) with functional streptavidin was performed as described in Supp. 5. The next step was injection biotin-EG<sub>8</sub>-Orai peptide aa 47-65 or aa 52-65 R52A R53A (2  $\mu$ M in Hepes buffer), in flow cell 1. Finally, the binding of CaM in Ca-free buffer or Ca-buffer was tested as described in Supp. 5. The sensorgrams show binding of CaM to peptide aa 47-65 (flow cell 1, solid black line) and to the corresponding peptide-free control cell (flow cell 2, dotted black line), as well as of CaM binding to peptide aa 52-65 R52A R53A (flow cell 1, solid red line) and to the corresponding peptide-free control cell (flow cell 2, dotted red line). The curves were vertically displaced by small increments to avoid overlap of the data.

**Supp. Fig. 6. Neither CRACR2A knock-down nor CRACR2A over-expression affects Orai3 gating.** a) Time-course of whole cell inward currents at -74 mV activated by passive store-depletion of HEK 293 cells coexpressing STIM1 and Orai1 together with either siRNA CRACR2A or CRACR2B in comparison to control siRNA. b) d) Time-course of whole cell inward currents at -74 mV activated by passive store-depletion of HEK 293 cells coexpressing STIM1 and b) Orai3 or d) Orai3  $\Delta$ N<sub>1-53</sub> together with either siRNA CRACR2A or CRACR2B in comparison to control siRNA. c) e) Corresponding, mean fast inactivation for 100 ms upon voltage steps from a holding potential of 0 mV to -90 mV of normalized current traces to b) d). f) h) Time-course of whole cell inward currents at -74 mV activated by passive store-depletion of HEK 293 cells coexpressing STIM1 and f) Orai3 or h) Orai3  $\Delta$ N<sub>1-53</sub> together with either CRACR2A or CRACR2B in comparison to control cells. g) i) Corresponding, mean fast inactivation for 100 ms upon voltage steps from a holding potential of 0 mV to -90 mV of normalized current traces to f) h).

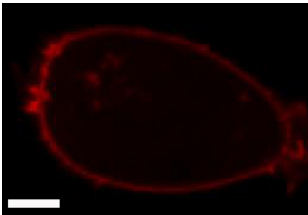
## Supplementary Figure 1

Orai1	66	lnehs	mcalswrkly	lsraklkass	rtsallsgfa	mvamvevqld
Orai2	40	snhhs	vcalswrkly	lsraklkass	rtsallsgfa	mvamvevqle
Orai3	41	asqhs	lralswrrly	lsraklkass	rtsallsgfa	mvamvevqle

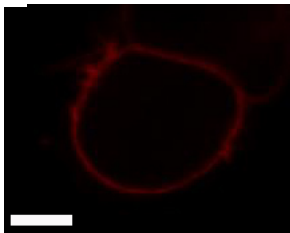
**CaM binding domain; conserved region; 1<sup>st</sup> transmembrane domain**

Supplementary Figure 2

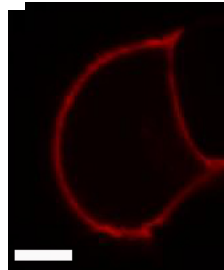
**a** Orai3 wild-type



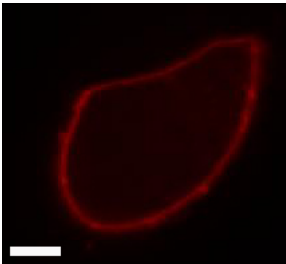
**b** Orai3  $\Delta N_{1-47}$



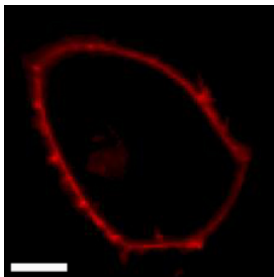
**c** Orai3  $\Delta N_{1-51}$



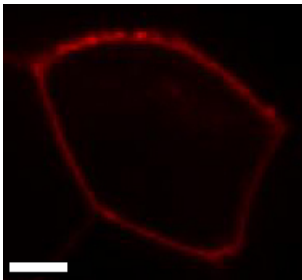
**d** Orai3  $\Delta N_{1-53}$



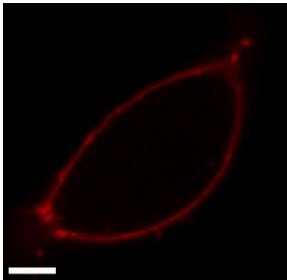
**e** Orai3  $\Delta N_{1-55}$



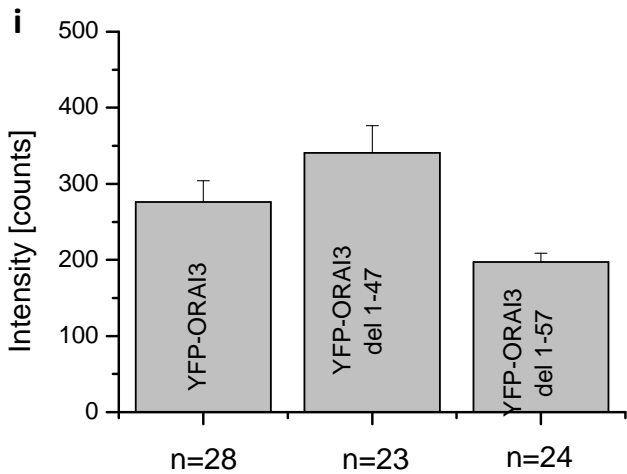
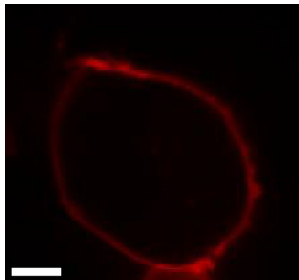
**f** Orai3  $\Delta N_{1-57}$



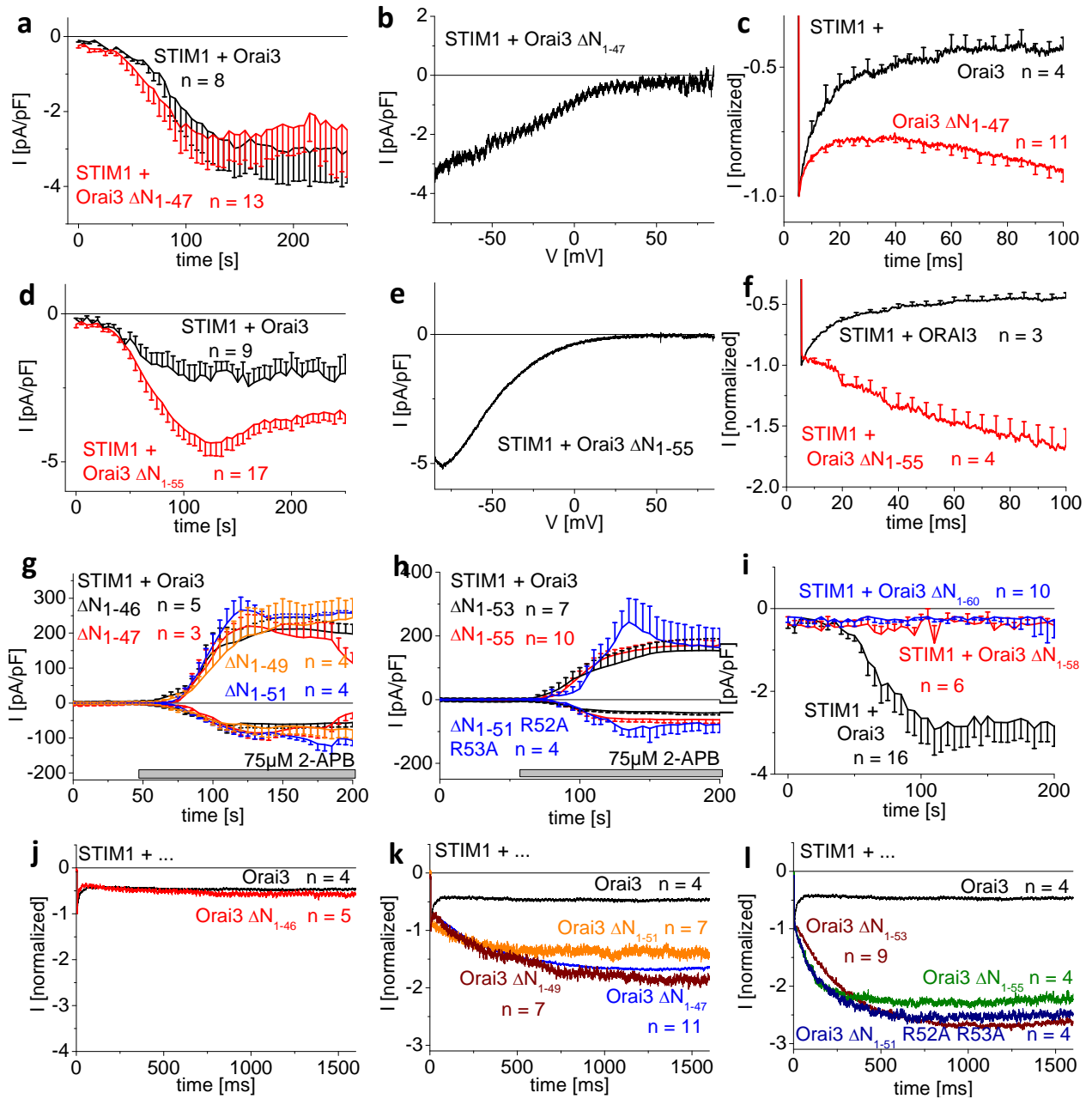
**g** Orai3  $\Delta N_{1-62}$



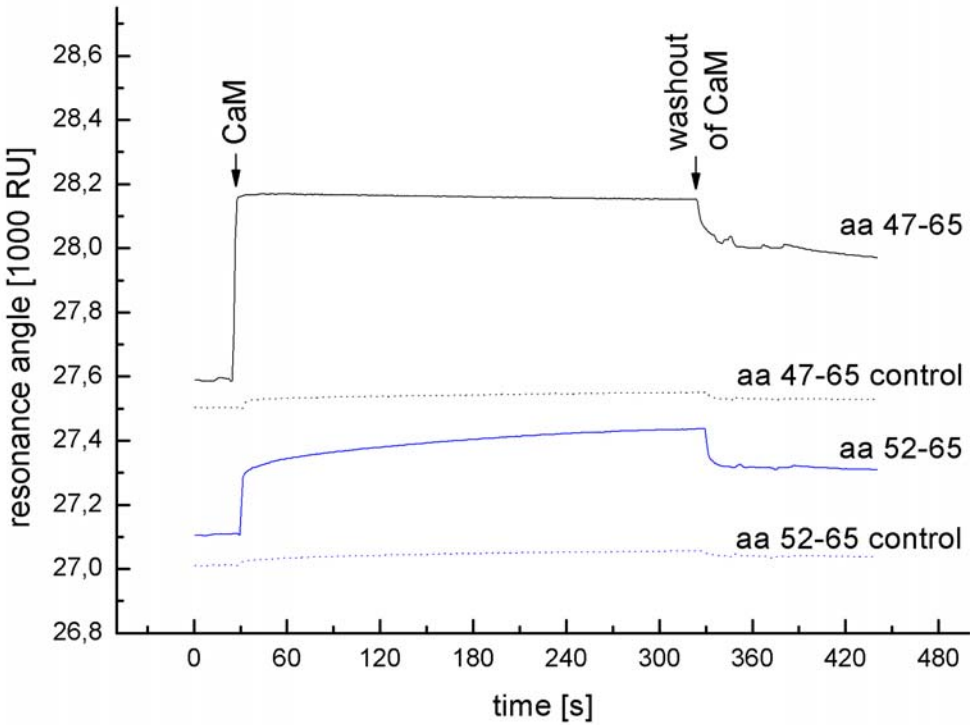
**h** Orai3  $\Delta N$ -term.



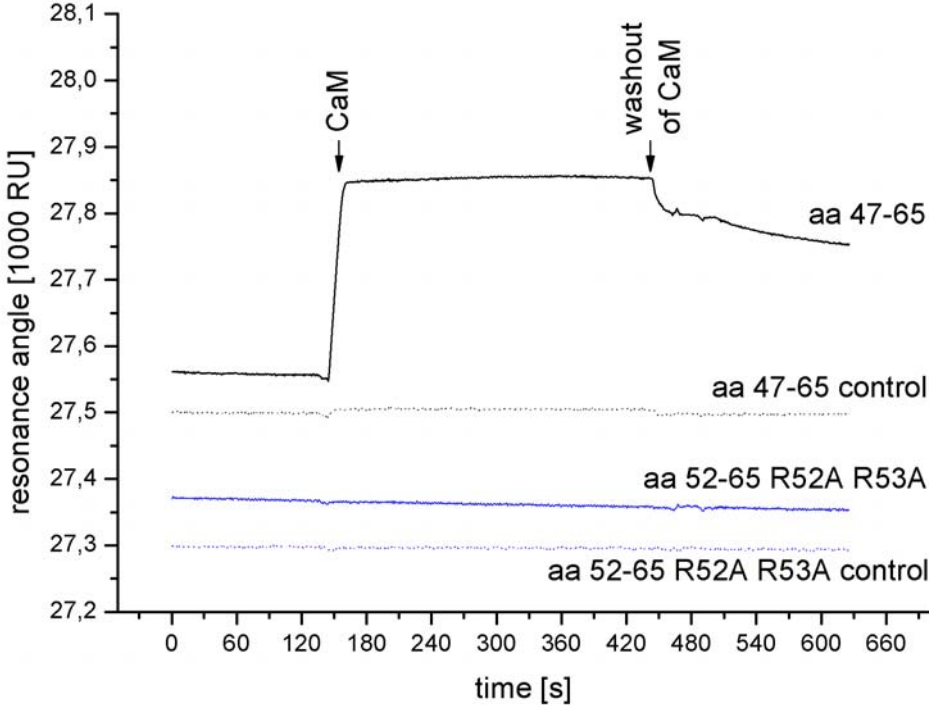
Supplementary Figure 3



Supplementary Figure 4



Supplementary Figure 5



Supplementary Figure 6

